applying (4.11) a second time. Unfortunately, there are 12 distinct possibilities for the order in which three components are combined, and each may yield decidedly different values of ϵ_{av} for the mixture! Even the Bruggeman formula, which does not distinguish between matrix and inclusion, yields slightly different results depending on the order in which the constituents are included.

In general, the Bruggeman formula tends to produce results that fall between the extremes of the various Maxwell Garnett combinations. Unfortunately, it is not obvious in most cases which, if any, of the many possibilities is "best."

Ultimately, any formula for the effective dielectric constant of a heterogeneous mixture is derived based on approximations or assumptions that may or may not be valid for the case under consideration. Wherever possible, the chosen method should be validated for the application in question by comparing predictions with actual measurements.

4.2 Refraction and Reflection

When an EM wave encounters a planar boundary between two homogeneous media having different indices of refraction, some of the energy of the wave is *reflected*, while the remainder passes through the boundary into the second medium (Fig. 4.3b, Fig. 4.4). In addition, the direction of the transmitted wave in medium 2 may be altered from the original direction in medium 1, a phenomenon known as *refraction* (Fig. 4.3a). The nature of both reflection and refraction at an interface between two homogeneous media follows directly from Maxwell's equations, combined with appropriate continuity constraints imposed at the boundary, and is covered extensively in other texts. We will not repeat the derivations here but simply summarize the key results.

4.2.1 Angle of Reflection

Consider an EM wave incident on a plane interface between two media. If the local normal unit vector is $\hat{\mathbf{n}}$ and the direction of the incident ray is $\hat{\mathbf{\Omega}}_i$, then the reflected ray $\hat{\mathbf{\Omega}}_r$ lies in the same plane as $\hat{\mathbf{n}}$ and $\hat{\mathbf{\Omega}}_i$ but on the opposite side from $\hat{\mathbf{\Omega}}_i$. Furthermore, the angle

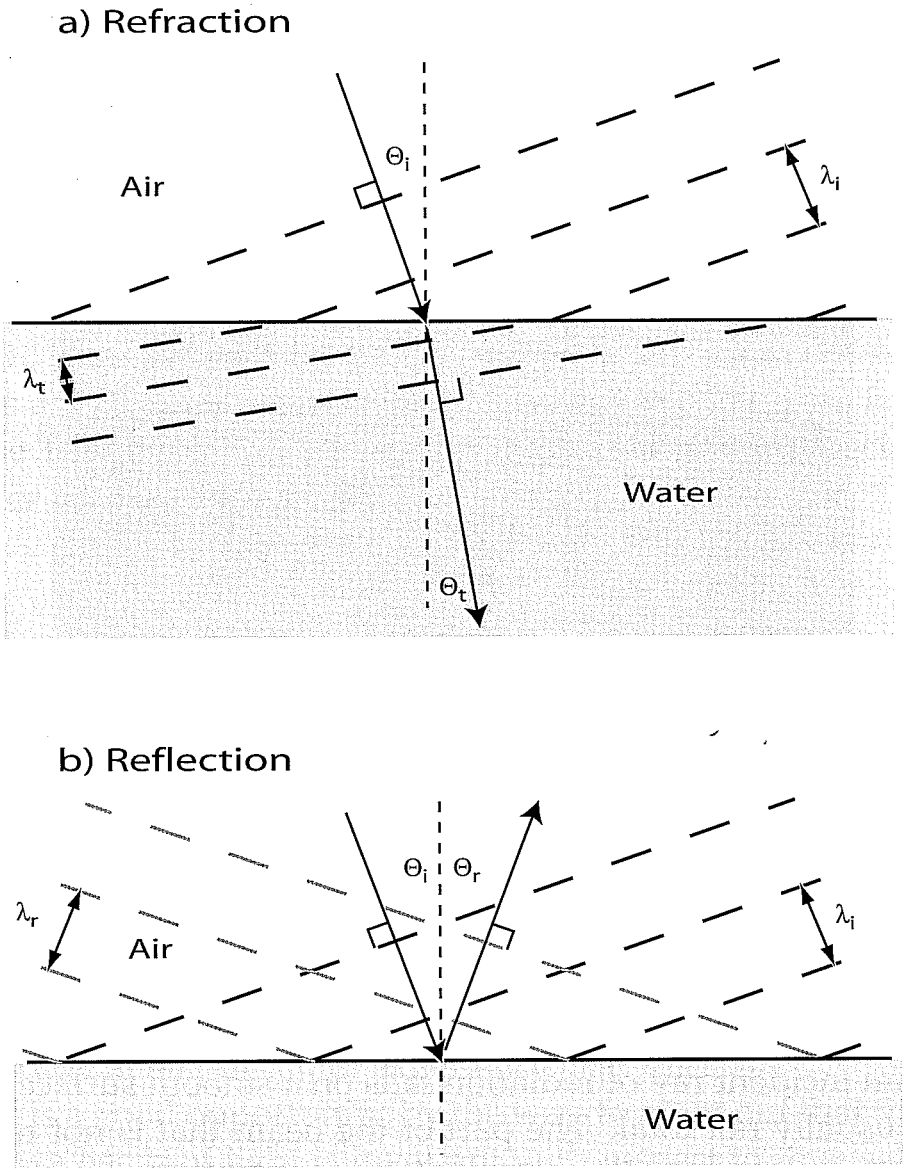

Fig. 4.3: Geometry of (a) refraction and (b) reflection of plane waves at an air-water interface.

Θ_r between $\hat{\mathbf{\Omega}}_r$ and $\hat{\mathbf{n}}$ equals the angle of incidence Θ_i defined by $\hat{\mathbf{n}}$ and $\hat{\mathbf{\Omega}}_i$.

In simple terms, a ray of light (or other EM radiation) reflects from a smooth surface much like an ideal elastic ball thrown at the floor: the component of its motion perpendicular to the surface abruptly reverses, while the component parallel to the surface remains unchanged. Reflection obeying this rule is termed *specular reflection.* The basic requirement in order for reflection to be specular is that any irregularities on the surface must be much smaller than the incident wavelength. In the visible band, this is generally

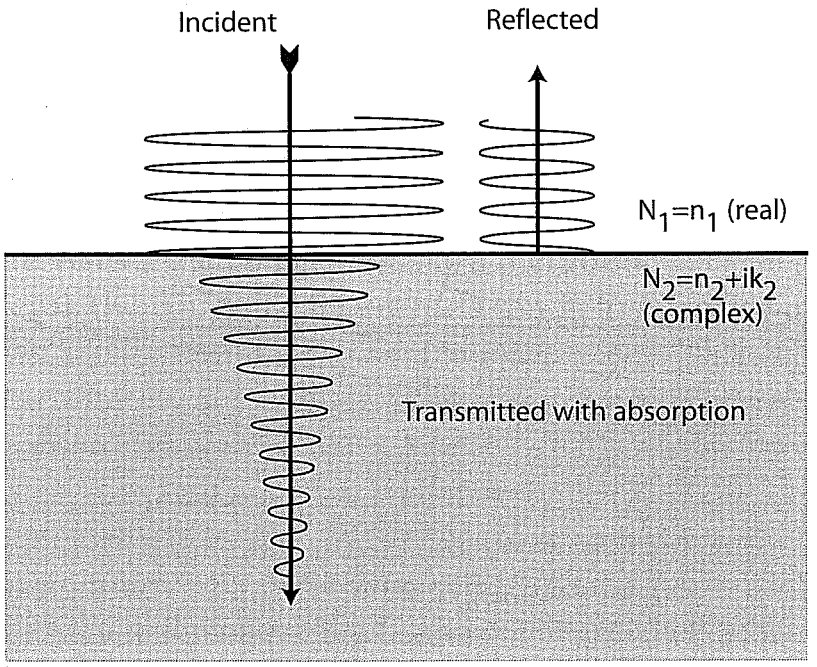

Fig. 4.4: Reflection and transmission of normally incident radiation.

true of glass, polished metals, most liquids (including water), and many plastic materials.

4.2.2 Angle of Refraction

When an incident ray of radiation falls on a smooth surface, reflection is usually not total. The part of the beam that is not reflected passes into the second medium. In general, the transmitted ray changes direction according to Snell's Law

$$\boxed{\frac{\sin\Theta_t}{N_1} = \frac{\sin\Theta_i}{N_2}\,,} \tag{4.13}$$

where N_1 and N_2 are the indices of refraction of the first and second medium, respectively, and Θ_t is the angle of the transmitted ray $\hat{\mathbf{\Omega}}_t$ relative to $\hat{\mathbf{n}}$. Although N_1 and/or N_2 may be complex, the above law is most easily interpreted when the both are real, or nearly so (i.e., weak absorption).

Case 1: $\Theta_i = \Theta_t = 0$. If a ray is normally incident on a surface, there is no change of direction as it enters the second medium.

Case 2: $\Theta_i > 0$; $N_2 > N_1$. A ray incident obliquely on a medium with larger index of refraction will bend *toward* the local normal; i.e., $\Theta_t < \Theta_i$. This situation describes sunlight falling on a smooth water surface, such as the surface of a pond or the exterior surface of a raindrop.

Case 3: $\Theta_i > 0$; $N_2 < N_1$. A ray incident obliquely on a medium with smaller index of refraction will bend *away* from normal; i.e., $\Theta_t > \Theta_i$. This situation arises, for example, when a ray of sunlight that has already entered a raindrop attempts to exit on the far side.

Case 3 above includes an interesting and important special case. Consider the possibility that

$$\Theta_i > \Theta_0 \,, \tag{4.14}$$

where the *critical angle* is defined as

$$\Theta_0 \equiv \arcsin\left(\frac{N_2}{N_1}\right) \,, \tag{4.15}$$

provided that $N_2 < N_1$. But (4.13) would then imply $\sin\Theta_t$ greater than one, a mathematical impossibility! The way out of this apparent paradox is to recognize that waves incident on the interface at an angle greater than the critical angle simply cannot pass through the interface at all but rather experience *total reflection*.

This is a good opportunity, by the way, to point out that the path taken by a beam of light is invariant with respect to reversal of direction. Viewed one way, Θ_0 defines the threshold for total internal reflection within the denser medium; viewed another, it describes the maximum possible value of Θ_t when light is externally incident on the medium at the largest possible angle ($\Theta_i = 90°$).

In the visible band, $N_1 \approx 1.33$ for water and $N_2 \approx 1$ for air; hence, in water, $\Theta_0 \approx 49°$.

Problem 4.2: Show that, for real N, Snell's Law (4.13) can be derived geometrically by requiring that the intersection of wave fronts with a planar boundary between two media match on both sides of the boundary (see Fig. 4.3).

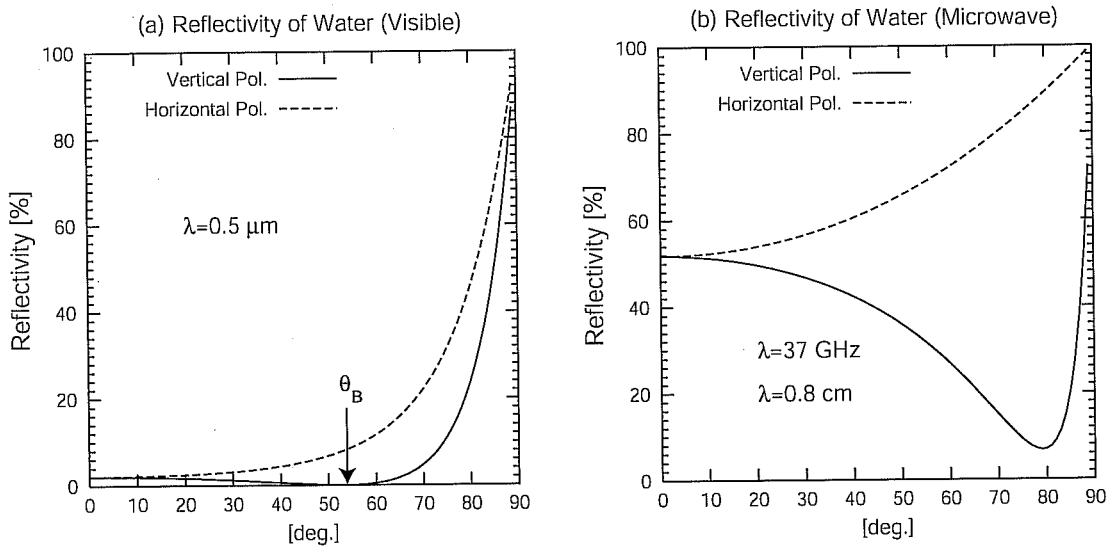

Fig. 4.5: Examples of the specular reflectivity of water as a function of incidence angle. (a) Visible band. (b) Microwave band.

4.2.3 Reflectivity

We have just addressed three aspects of how EM waves are affected by a planar interface between two homogeneous media: 1) the *angle of reflection* ($\Theta_i = \Theta_r$), 2) the *angle of refraction* (Snell's Law), and 3) the *critical angle for total reflection*. We now turn to the following slightly more complicated question: given that a beam of radiation is incident on a surface at an angle $\Theta_i < \Theta_0$, *what fraction of the beam is reflected?*

As before, the answer follows from the equations for a plane EM wave, with suitable constraints on the continuity of the magnetic and electric fields at the boundary. Also as before, we will not reproduce the derivation here but rather summarize the key results, in the form of the *Fresnel relations*:

$$R_p = \left| \frac{\cos\Theta_t - m\cos\Theta_i}{\cos\Theta_t + m\cos\Theta_i} \right|^2 , \tag{4.16}$$

$$R_s = \left| \frac{\cos\Theta_i - m\cos\Theta_t}{\cos\Theta_i + m\cos\Theta_t} \right|^2 , \tag{4.17}$$

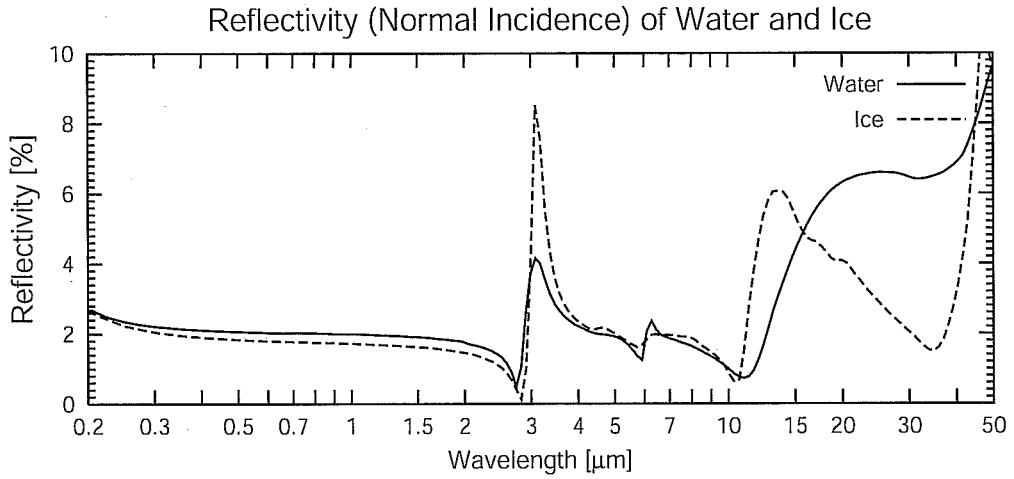

Fig. 4.6: The reflectivity (in air) of water and ice at normal incidence, based on (4.21) applied to the complex indices of refraction plotted in Fig. 4.1.

where Snell's Law can be manipulated to yield

$$\cos\Theta_t = \sqrt{1 - \left(\frac{\sin\Theta_i}{m}\right)^2}, \tag{4.18}$$

and the complex *relative index of refraction* m is defined as

$$\boxed{m = \frac{N_2}{N_1}\,.} \tag{4.19}$$

R_p and R_s are *reflectivities*. They give the fraction of an incident beam of radiation that is reflected from a smooth interface, given the local angle of incidence Θ_i and the relative index of refraction m.

But why do we have *two* expressions for reflectivity? It turns out that this is one of those cases when the *polarization* of the incident radiation matters. R_p defines the reflectivity when the electric field vector is parallel to the plane of incidence; R_s is valid when the electric field vector is perpendicular to the plane of incidence. Since any EM wave can be decomposed into parallel and perpendicular polarized components, the total reflectivity can always be found by taking an appropriate average of R_p and R_s. For example, if the incident radiation happens to be unpolarized, then parallel

and perpendicular polarizations are present in equal amounts, in which case the total reflectivity is given by

$$\boxed{R = \frac{1}{2}(R_s + R_p)\ .} \tag{4.20}$$

Note, however, that the reflected radiation is, in general, no longer unpolarized, so it can be dangerous to disregard polarization when considering the net outcome of multiple reflections from surfaces.

For the special case that $\Theta_i = 0$, both (4.16) and (4.17) collapse to the following single expression for the *reflectivity at normal incidence*:

$$\boxed{R_{\text{normal}} = \left|\frac{m-1}{m+1}\right|^2\ .} \tag{4.21}$$

At normal incidence, there is no physically important distinction between the two polarizations, hence the need for only one formula.

In atmospheric applications, smooth reflecting surfaces are often horizontal, the most common example being a water surface, such as the ocean or a lake. In this case, parallel polarization is often known as *vertical polarization*, and perpendicular polarization equates to *horizontal polarization*. The corresponding reflectivities are then written as R_v and R_h. This terminology is common in the field of microwave remote sensing, where the rather large difference between R_v and R_h is of great practical importance. Figure 4.5a gives examples of R_v and R_h as functions of incidence angle for water in the visible band. The following features are of particular interest:

- In general, the reflectivity is quite low (2%) for light at near-normal incidence ($\Theta_i \approx 0$) but increases sharply to 100% for near-grazing angles ($\Theta_i \to 90°$). In other words, a smooth water surface is a rather poor reflector of sunlight at high noon but an excellent reflector of the setting sun. This is of course consistent with everyday experience.

- Except at near-grazing and near-normal incidence, the reflectivity for vertical polarization is much lower than that for horizontal polarization. It is this fact that led to the development of polarizing sunglasses, which block the largely horizontally polarized glare from water and other reflecting surfaces while transmitting vertically polarized light from other sources.

- There is a single angle Θ_B, known as the *Brewster angle*, at which the reflectivity for vertically polarized radiation vanishes completely, implying that *only* the horizontally polarized component of incident light survives reflection at that angle. By setting the numerator in (4.16) equal to zero and solving for $\sin\Theta_i$, we find that

$$\boxed{\Theta_B = \arcsin\sqrt{\frac{m^2}{m^2+1}}\,.} \tag{4.22}$$

  For water in the visible band, the $\Theta_B = 53°$.

All of the above features can be found in the reflectivities of most nonconducting materials; i.e., those for which n_i is zero or at least very small. Larger values of the real part of m lead to greater overall reflectivities, larger values for the Brewster angle Θ_B, and smaller values for the critical angle for total internal reflection Θ_0. Diamonds, with their unusually large $N = 2.42$, owe their alluring sparkle to all three properties.

Problem 4.3: For (a) glass with $N = 1.5$ and (b) a diamond with $N = 2.42$, find the values of the reflectivity at normal incidence, and the critical angle for total internal reflection Θ_0. In both cases, assume that the external medium is air, with $N \approx 1.0$. Compare your results with their counterparts for water.

In the case of conducting materials, e.g., metals, as well as liquid water at microwave frequencies (Fig. 4.5b), the imaginary part of m is significantly greater than zero and also contributes to increased

reflectivity. However, although the vertically polarized reflectivity still has a minimum at some angle Θ_B, that minimum is no longer zero. Therefore, (4.22) cannot be used to find Θ_B in such cases.

4.3 Applications to Meteorology, Climatology, and Remote Sensing

4.3.1 Rainbows and Halos

Geometric Optics

In the previous section, we tacitly assumed that we were dealing with EM waves incident on a *planar* (flat) boundary between two homogeneous media. However, the above rules for reflection and refraction can be applied not only to planar boundaries, but to any surface whose radius of curvature is much greater than the wavelength of the radiation. In this case, the angles Θ_i, Θ_t, Θ_r, Θ_0, etc., are measured relative to the local normal where the ray intercepts the surface. With this generalization, we have the ability to analyze the scattering and absorption properties of a variety of atmospheric hydrometeors via the straightforward technique of *ray tracing*, also known as *geometric optics*.

Unfortunately, most particles in the atmosphere are not much larger, and may even be smaller, than the wavelength of interest. This is true for air molecules, aerosols and cloud droplets in the visible and infrared bands and even raindrops in the microwave band. Geometric optics cannot be used for these cases; rather, more sophisticated solutions to the wave equation must be derived. These solutions and their interpretation will be outlined in Chapter 12.

Nevertheless, there are a number of interesting cases for which the particle size *is* much larger than the wavelength. This condition applies for example to the scattering of visible sunlight ($\lambda < 0.7$ μm) by large cloud ice particles (>50 μm) and raindrops (100 μm $< r <$ 3 mm). In fact, a number of common optical phenomena, such as rainbows, halos, and parhelia (sundogs) can be explained by geometric optics, simply by considering how rays of light refract and reflect as they encounter the surface of the particle.

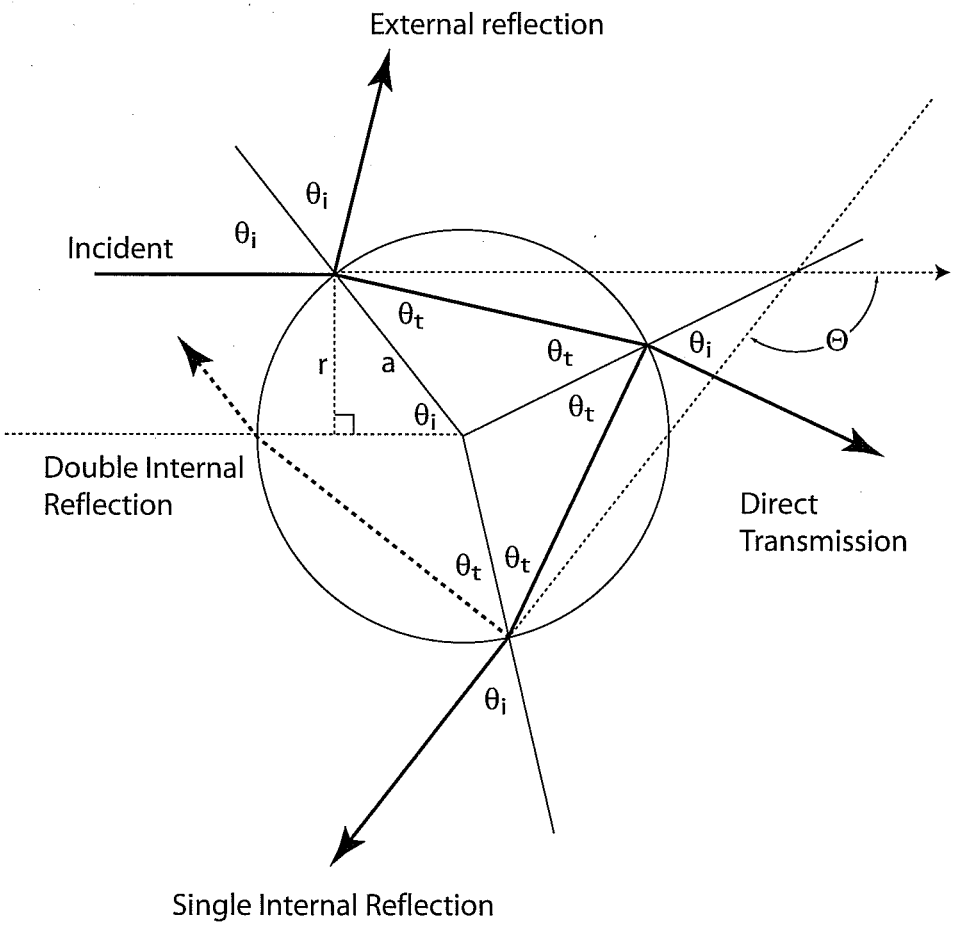

Fig. 4.7: Ray tracing geometry for a spherical water droplet of radius a, for a ray incident at distance r from a parallel line passing through the drop center. θ_i and θ_t denote the incident and transmitted angles relative to the local normal and are related by Snell's law. Θ is the angle of scattering relative to the original direction of the ray, in this case for a ray that has undergone a single internal reflection.

The Rainbow

To a reasonable approximation, a falling raindrop is spherical. If a spherical droplet is uniformly illuminated, then the geometry of the path of each incident ray depends only on $x \equiv r/a$, where r is the distance of the incident ray from the center axis of the drop, and a is the radius of the drop (Fig. 4.7). So $x = 0$ corresponds to a ray that is incident "dead center," while $x = 1$ corresponds to a ray that barely grazes the edge of the sphere.

Now let's follow the path of a single incident ray after it intercepts the drop:

1. A fraction of the energy in the ray will be reflected upon its

first encounter with the surface of the drop. If the incident radiation is unpolarized, then that fraction will be given by the average of the Fresnel relations (4.16) and (4.17), evaluated for the local angle of incidence θ_i. Fig. 4.5 reveals that this fraction is typically only a few percent, except when the ray strikes the sphere at a near-grazing angle.

2. Whatever is not reflected is transmitted into the drop and refracted to an angle θ_t relative to the local normal, as required by Snell's Law.

3. The above ray now encounters the back side of the drop, where a small fraction (a few percent) is reflected internally, as determined again by the Fresnel relations. The remainder exits the drop again at an angle θ_i relative to the local normal.

4. That portion of the original ray that was internally reflected now encounters the surface from the inside again. As before, a fraction is reflected internally (now for a second time), while the remainder is transmitted to the exterior. It is the part that escapes at this point that is responsible for the primary rainbow.

5. The above process is repeated for each additional internal reflection. However, after only two internal reflections, very little of the original energy in the incident ray remains inside the drop. The part that exits the drop after exactly two internal reflections is responsible for the secondary rainbow.

As noted above, the primary rainbow is associated with radiation that undergoes a single internal reflection before exiting the droplet again, so let's take a closer look at that case. Figure 4.8a depicts the full range of possible paths for rays undergoing a single internal reflection. If the incident ray encounters the droplet dead center ($x = 0$), it of course gets reflected exactly backward from the rear surface of the drop, so the scattered direction for that ray is 180°. A ray that encounters the droplet just slightly off-axis will undergo a slight degree of refraction, reflect off the rear surface at a slightly non-normal angle, and ultimately exit the drop at an angle near to, but not quite equal to 180°.

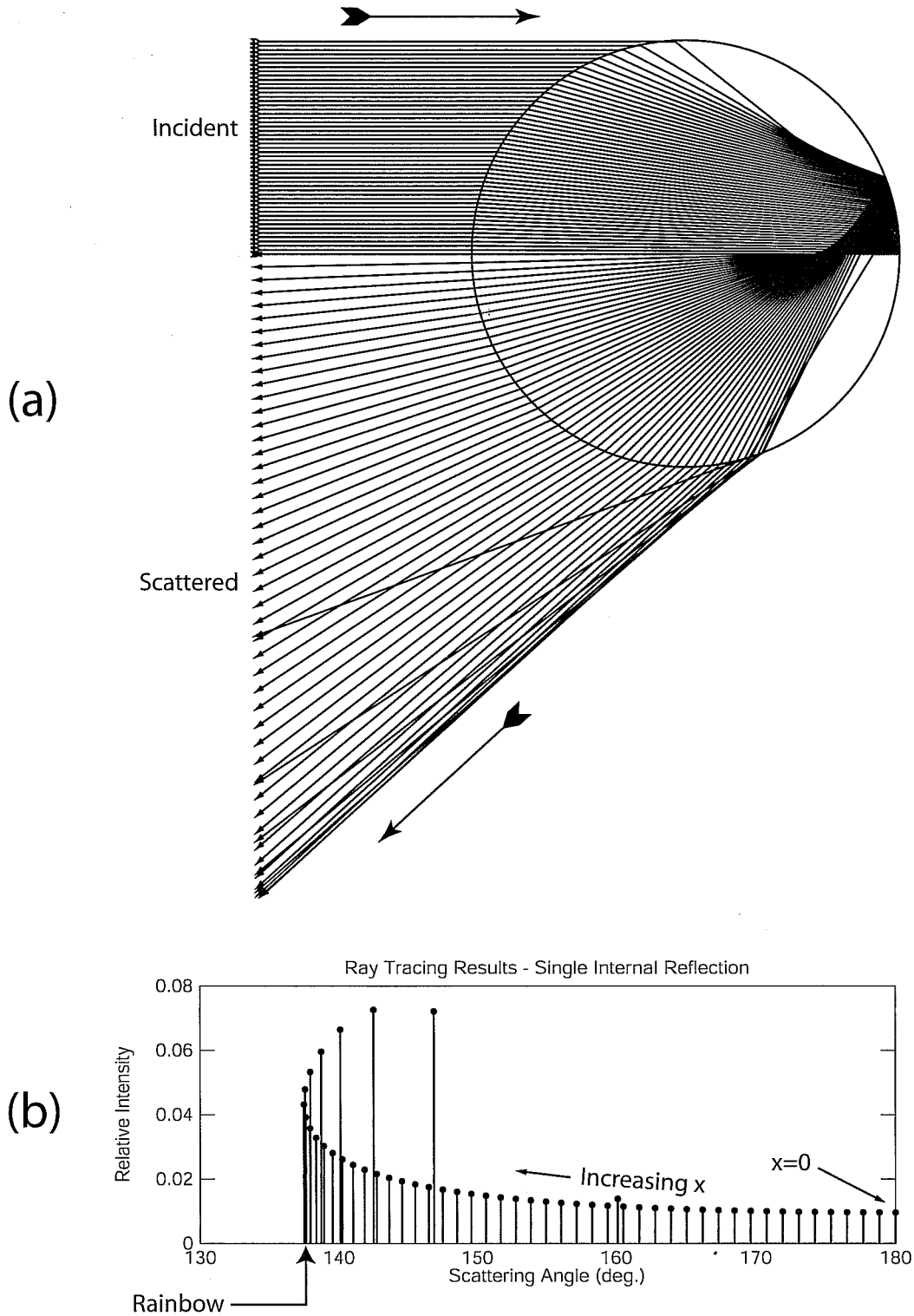

Fig. 4.8: Illustration of the ray-tracing method applied to a spherical water drop. (a) Diagram tracing the rays that undergo a single internal reflection, assuming uniform incident illumination. (b) Angles and relative intensities of the scattered rays.

Starting at $\Theta = 180°$ on the right edge of the plot in panel (b), we see how Θ for each subsequent ray (increasing x) initially decreases at a fairly steady rate. Also shown is the relative intensity of the exiting ray, based on the fraction that "survives" this particular path according to the Fresnel relations. The overall intensity in a particular direction is proportional to the intensity of the individual rays times the density of rays per increment of Θ.

Although the trend initially is toward ever-smaller Θ, there comes a point where Θ reaches a minimum, which we'll call Θ_0, and starts increasing again. For water, which has an index of refraction of approximately 1.33 in the visible band, $\Theta_0 \approx 137°$.

Because the reversal is gradual, there is a fairly significant range of x for which the scattered rays all bunch up rather close to Θ_0. It is this "focusing" of energy on a narrow range of Θ that gives rise to the bright ring that we call a rainbow. Of course, a rainbow is only visible when a rainshower is illuminated by a directional source of bright light — e.g., sunlight.

The precise value of Θ_0 depends of course on the index of refraction: increasing n_r has the effect of increasing Θ_0. A rainbow exhibits the characteristic separation of colors for which it is best known because n_r for water increases slightly from the red end to the violet end of the visible spectrum (Fig. 4.1).

As already mentioned, a similar process is behind the much weaker secondary rainbow, which arises from two internal reflections. The scattering angle for the second rainbow is approximately 130°, which puts it about 7° outside the primary rainbow, when you are viewing it with the sun at your back.

Halos and Related Optical Phenomena

Ray tracing can also be used to explain optical features like *halos*, which are bright rings that appear around the sun in conjunction with a thin cirrostratus cloud layer, and *parhelia* (or sundogs), which are bright iridescent spots positioned on either side of the sun, usually in connection with cirrus clouds, when the sun is fairly low in the sky. In both cases, the most common angle separating the halo or parhelion from the sun is 22°. This scattering angle is associated with refraction (without internal reflection) through two

faces of a hexagonal ice crystal whose extensions form a 60° angle.

In contrast to the case for the rainbow, ray tracing analysis of various optical phenomena associated with ice crystals is complicated by the fact that they are not spherical. Therefore, results for all possible orientations of the crystal must be obtained and then averaged together. Halos are associated with randomly oriented crystals, but most other optical phenomena in cirrus clouds, including sundogs, require ice crystals falling with a preferred orientation.

A fuller discussion of the optics of rainbows and haloes may be found in BH83, section 7.2 and 7.3, and L02, section 5.3.